Valence quark distributions in mesons in generalized QCD sum rules.

B.L.Ioffe*and A.G.Oganesian†
Institute of Theoretical and Experimental Physics,
B.Cheremushkinskaya 25, 117218 Moscow,Russia

Abstract

The method for calculation of valence quark distributions at intermediate x is presented. The imaginary part of the virtual photon forward scattering amplitude on the quark current with meson quantum number is considered. Initial and final virtualities p_1^2 and p_2^2 of the currents are assumed to be large, negative and different, $p_1^2 \neq p_2^2$. The operator product expansion (OPE) in p_1^2, p_2^2 up to dimension 6 operators is performed. Double dispersion representations in p_1^2, p_2^2 of the amplitude in terms of physical states contributions are used. Equalling them to those calculated in QCD by OPE the desired sum rules for quark distributions in mesons are found. The double Borel transformations are applied to the sum rules, killing non-diagonal transition terms, which deteriorated the accuracy in the previous calculations of quark distributions in nucleon. Leading order perturbative corrections are accounted. Valence quark distributions in pion, longitudinally and transversally polarized ρ-mesons are calculated at intermediate x, $0.2 \lesssim x \lesssim 0.7$ and normalization points $Q^2 = 2 - 4\ GeV^2$ with no fitting parameters. The use of the Regge behaviour at small x and quark counting rules at large x allows one to find the first and the second moments of valence quark distributions. The obtained quark distributions may be used as an input for evolution equations. In the case of pion the quark distribution is in agreement with those found from the data on the Drell-Yan process. Quark distributions in transversally and longitudinally polarized ρ-mesons are essentially different.

*Email address: ioffe@vitep5.itep.ru
†Email address: armen@vitep5.itep.ru

1 Introduction

Quark and gluon distributions in hadrons are not calculated in QCD starting from the first principles. What is only possible is to calculate their evolution with Q^2. In the case of nucleon the standard way is the following. At some fixed $Q^2 = Q_0^2$ the form of quark and gluon distributions, characterized by the number of free parameters is assumed. Then the evolution of distributions with Q^2 is calculated and after comparing with the data of the deep inelastic lepton-nucleon scattering the best fit for these parameters is found. (About dozen of the parameters is used, see, e.g. the recent papers [1]-[4]). Quark and gluon distributions in pions are determined in a similar way from the data on production of e^+e^- and $\mu^+\mu^-$ pairs in pion-nucleon collisions (the Drell-Yan process) [5, 6] and prompt photons production [7]. But here one needs an additional hypothesis about connection of the fragmentation function at time-like Q^2, which is measured in the Drell-Yan processes, with parton distributions defined at space-like Q^2. For other mesons and baryons, as well as for unmeasured up to now distributions in polarized nucleon (like $h_1(x)$) we have no information about parton distributions from experiment and have to rely on models. The QCD calculation of quark and gluon distributions in hadrons, which could be used as an input in evolution equations may be considered as a challenge for the theory.

The method of valence quark distributions calculation at intermediate x was suggested in [8] and developed in [9]-[11]. The idea was to consider the imaginary part (in s-channel) of 4-point correlator, corresponding to the forward scattering of two-quark currents, one of which has the quantum numbers of hadron of interest and the other is electromagnetic (or weak). It was supposed that virtualities of the photon and hadronic current q^2 and p^2 are large and negative $|q^2| \gg |p^2| \gg R_c^{-2}$, where R_c is the confinement radius (q is the momentum of virtual photon, p is the momentum, carried by hadronic current). It was shown [9], that in this case the imaginary part in s channel $[s = (p+q)^2]$ of the forward scattering amplitude is dominated by small distance contributions at intermediate x. (The standard notation is used: x is the Bjorken scaling variable , $x = -q^2/2\nu,\ \nu = pq$). The proof of this statement, given in [9], is based on the fact that for the imaginary part of the forward scattering amplitude the position of the closest to zero singularity in momentum transfer is determined by the boundary of the Mandelstam spectral function and is given by the equation

$$t_0 = -4\frac{x}{1-x}p^2 \tag{1}$$

Therefore, if $|p^2|$ is large and x is not small, then even at $t = 0$ (the forward amplitude) the virtualities of intermediate states in t-channel are large enough for OPE to be applicable. The further procedure is common for the QCD sum rules. On one side, the amplitude is calculated by OPE with the account of condensates. On the other side, the dispersion representation in p^2 in terms of physical states is written for the same amplitude and the contribution of the lowest state is extracted by using the Borel transformation. As follows from (1), the approach is invalid at small x. (Since in real calculations $-p^2$ are of order $1 - 2\ GeV^2$, small x means in fact $x \lesssim 0.1 - 0.2$). This statement is evident *apriori*, because at small x Regge behaviour is expected, which cannot be described in the framework of OPE. The approach is also invalid at x close to 1. This is the domain of resonances, also outside the scope of OPE. The fact that this method of calculation of quark distributions in hadrons is invalid at $x \ll 1$ and at $1 - x \ll 1$ follows from the theory itself: the OPE diverges in these two

domains. Therefore, calculating higher order terms of OPE makes it possible to estimate up to which numerical values of x, in the small and large x domain, the theory is reliable in each particular case. In the way described above, valence quark distributions in nucleon [9, 11] were calculated. However, the accuracy of the calculation was not good enough, especially for d-quarks [9]. Moreover, it was found to be impossible to calculate quark distributions in π- and ρ-mesons in this way. The reason is that the sum rules in the form used in [9, 11] have a serious drawback. (The calculation of the photon structure function [10] is a special case and has no such problem).

The origin of this drawback comes from the fact that in the case of 4-point function, which corresponds to the forward scattering amplitude with equal inital and final hadron momenta, the Borel transformation does not provide suppression of all excited state contributions: the non-diagonal matrix elements, like

$$\langle 0|j^h|h^*\rangle\langle h^*|j^{el}(x)j^{el}(0)h\rangle\langle h|j^h|0\rangle \tag{2}$$

are not suppressed in comparison with the matrix element of interest

$$\langle 0|j^h|h\rangle\langle h|j^{el}(x)j^{el}(0)|h\rangle\langle h|j^h|0\rangle \tag{3}$$

proportional to the hadron h structure function. (Here h is the hadron which structure function we would like to calculate, h^* is the excited state with the same quantum numbers as h, j^h is the quark current with quantum numbers of hadron h, j^{el} is the electromagnetic current). In order to kill the background matrix elements (2) it was necessary to differentiate the sum rule over the Borel parameter. But, as is well known, differentiation of an approximate relation may seriously deteriorate the accuracy of the results. In QCD sum rules such differentiation increases contributions of higher order terms of OPE and excited states in physical spectrum, the sum rules become much worse or even fail (as for π and ρ-mesons). For pion the situation is especially bad, because direct calculation show, that the leading term in OPE (the bare loop diagram) corresponds just to the non-diagonal matrix element, not to the pion structure function.

In ref.12 it was suggested the modified method of calculation of the hadron structure functions (quark distributions in hadrons), where this problem is eliminated and valence quark distributions in pion were calculated. This method is used here for calculation of valence quark distributions in ρ-meson, separately for longitudinally and transversally (relative to the virtual photon beam) polarized ρ-mesons. Since quark distributions in ρ-meson cannot be measured experimentally, the common way to get them is to assume SU(6) symmetry, where π- and ρ-mesons belong to the same multiplet. Then quark distributions in ρ-meson are equal to that in pion and are independent on ρ polarization. On the other side, the pion play a specific role in the theory – it is a Goldstone boson. From this point of view it has nothing in common with ρ-meson and there are no reasons to expect, that quark distributions in π and ρ are equal. This problem will be resolved and it will be shown, that valence quark distributions in pion, longitudinally and transversally polarized ρ-mesons are quite different.

For reader convenience we present first shortly the method of [12] and the results for quark distributions in pion. Then valence quark distributions in longitudinal and transverse ρ mesons are calculated. The valence quark distributions are reliably calculated in the domain of intermediate x, $\quad 0.2 \lesssim x \lesssim 0.65$. The use of the Regge behaviour at small x and quark

counting rules at large x allows one to find the first and the second moments of quark distributions.

2 The method

Consider the non-forward 4-point correlator:

$$\Pi(p_1,p_2;q,q') = -i\int d^4xd^4yd^4z e^{ip_1x+iqy-ip_2z} \times \langle 0|T\left\{j^h(x),\ j^{el}(y),\ j^{el}(0),\ j^h(z)\right\}|0\rangle \tag{4}$$

Here p_1 and p_2 are the initial and final momenta carried by hadronic current j^h, q and $q'=q+p_1-p_2$ are the initial and final momenta carried by virtual photons. (Lorenz indeces are omitted). It will be very essential for us to consider non-equal p_1,p_2 and treat p_1^2,p_2^2 as two independent variables. However, we may put $q^2=q'^2=q^2$ and $t=(p_1-p_2)^2=0$. We are interested in imaginary part of $\Pi(p_1^2,p_2^2,q^2,s)$ in s channel:

$$Im\Pi(p_1^2,p_2^2,q^2,s) = \frac{1}{2i}\left[\Pi(p_1^2,p_2^2,q^2,s+i\varepsilon) - \Pi(p_1^2,p_2^2,q^2,s-i\varepsilon)\right] \tag{5}$$

In order to construct representation of $Im\Pi(p_1^2,p_2^2,q^2,s)$ in terms of contributions of physical states, let us write for $Im\Pi(p_1^2,p_2^2,q^2,s)$ the double dispersion relation in p_1^2,p_2^2:

$$Im\Pi(p_1^2,p_2^2,q^2,s) = a(q^2,s) + \int\limits_0^\infty \frac{\varphi(q^2,s,u)}{u-p_1^2}du + \int\limits_0^\infty \frac{\varphi(q^2,s,u)}{u-p_2^2}du + \int\limits_0^\infty du_1 \int\limits_0^\infty du_2\ \frac{\rho(q^2,s,u_1,u_2)}{(u_1-p_1^2)(u_2-p_2^2)} \tag{6}$$

The second and the third terms in the right-hand side (rhs) of (6) may be considered as subtraction terms to the last one – the properly double spectral representation. The first term in the rhs of (6) is the subtraction term to the second and third ones. Therefore, (6) has the general form of the double spectral representation with one subtraction in both variables – p_1^2 and p_2^2. Apply the double Borel transformation in p_1^2,p_2^2 to (6). This transformation kills three first terms in rhs of (6) and we have

$$\mathcal{B}_{M_1^2}\mathcal{B}_{M_2^2}\ Im\Pi(p_1^2,p_2^2,q^2,s) = \int\limits_0^\infty du_1 \int\limits_0^\infty du_2 \rho(q^2,s,u_1,u_2) exp\left[-\frac{u_1}{M_1^2}-\frac{u_2}{M_2^2}\right] \tag{7}$$

The integration region over u_1,u_2 may be divided into 4 areas (Fig.1):

I. $u_1<s_0;\ \ u_2<s_0$

II.$u_1<s_0;\ \ u_2>s_0$

III. $u_1>s_0;\ \ u_2<s_0$

IV. $u_1,u_2>s_0$

Using the standard QCD sum rule model of hadronic spectrum and the hypothesis of quark-hadron duality, i.e. the model with one lowest resonance plus continuum, one may

clearly see, that area I corresponds to resonance contribution. Spectral density in this area can be written as

$$\rho(u_1, u_2, x, Q^2) = g_h^2 \cdot 2\pi F_2(x, Q^2)\delta(u_1 - m_h^2)\delta(u_2 - m_h^2), \tag{8}$$

where g_h is defined as

$$\langle 0|j_h|h\rangle = g_h \tag{9}$$

(For simplicity we consider the case of the Lorenz scalar hadronic current. The necessary modifications for cases of π and ρ-mesons will be presented below). If in $Im\Pi(p_1, p_2, q, q')$ the structure, proportional to $P_\mu P_\nu$ $[P_\mu = (p_1 + p_2)_\mu/2]$ is considered, then in the lowest twist approximation $F_2(x, Q^2)$ is the structure function depending on the Bjorken scaling variable x and weakly on $Q^2 = -q^2$.

In area (IV), where both variables $u_{1,2}$ are far from resonance region, the non-perturbative effects may be neglected, and as usual in sum rules, the spectral function of hadron state is described by the bare loop spectral function ρ^0 in the same region

$$\rho(u_1, u_2, x) = \rho^0(u_1, u_2, x) \tag{10}$$

In areas (II),(III) one of the variables is far from the resonance region, but other is in the resonance region, and the spectral function in this region is some unknown function $\rho = \psi(u_1, u_2, x)$, which corresponds to transitions like $h \to continuum$ as shown in Fig.2. After double Borel transformation the physical side of the sum rule can be written as (M_1^2, M_2^2 are Borel mass square)

$$\hat{B}_1\hat{B}_2[Im\Pi] = 2\pi F_2(x, Q^2) \cdot g_h^2 e^{-m_h^2(\frac{1}{M_1^2}+\frac{1}{M_2^2})} + \int\limits_0^{s_0} du_1 \int\limits_{s_0}^{\infty} du_2 \psi(u_1, u_2, x) e^{-(\frac{u_1}{M_1^2}+\frac{u_2}{M_2^2})}$$

$$+ \int\limits_{s_0}^{\infty} du_1 \int\limits_0^{s_0} du_2 \psi(u_1, u_2, x) e^{-(\frac{u_1}{M_1^2}+\frac{u_2}{M_2^2})} + \int\limits_{s_0}^{\infty}\int\limits_{s_0}^{\infty} du_1 du_2 \rho^0(u_1, u_2, x) e^{-(\frac{u_1}{M_1^2}+\frac{u_2}{M_2^2})} \tag{11}$$

In what follows we put $M_1^2 = M_2^2 \equiv 2M^2$. (As was shown in [13], the values of Borel parameters M_1^2, M_2^2 in the double Borel transformation are about twice of that in the ordinary ones).

One of advantages of this method is that after double Borel transformation unknown contribution of (II), (III) areas [the second and third term in (11)] are exponentially suppressed. Using duality arguments, we estimate the contribution of all non-resonancee region (i.e. areas II, III, IV) as a contribution of bare loop in the same region and demand their value to be small (less than 30%). So, equating physical and QCD representation of Π and taking into account cancellation of appropriate parts in the left and right sides, one can write the following sum rules:

$$Im\ \Pi^0_{QCD} + \text{Power}\ \ \text{correction} = 2\pi F_2(x, Q^2) g_h^2 e^{-m_h^2(\frac{1}{M_1^2}+\frac{1}{M_2^2})}$$

$$Im\Pi^0_{QCD} = \int\limits_0^{s_0}\int\limits_0^{s_0} \rho^0(u_1, u_2, x) e^{-\frac{u_1+u_2}{2M^2}} \tag{12}$$

It can be shown (see below), that for box diagram $\psi(u_1, u_2, x)) \sim \delta(u_1 - u_2)$, and, as a consequence, the second and third terms in (11) are zero in our model of hadronic spectrum.

It is worth mentioning that if we would consider the forward scattering amplitude from the beginning, put $p_1 = p_2 = p$ and perform Borel transformation in p^2, then unlike (11), the contributions of the second and third terms in (6) would not be suppressed comparing with the interesting for us lowest resonance contribution. They just correspond to the non-diagonal transition matrix elements discussed in the Introduction and are proportional to

$$\langle 0|j^h|h^*\rangle \ \frac{1}{p^2 - m_h^{*2}} \ \langle h^*|j^{el}(x)j^{el}(0)|h\rangle \ \frac{1}{p^2 - m_h^2}\langle h|j^h|0\rangle \tag{13}$$

From decomposition

$$\frac{1}{p^2 - m_h^{*2}} \ \frac{1}{p^2 - m_h^2} = \frac{1}{m_h^{*2} - m_h^2}\left(\frac{1}{p^2 - m_h^{*2}} - \frac{1}{p^2 - m_h^2}\right) \tag{14}$$

it is clear that in this case (13) may contribute to the second (or third) term in (6) and after Borel transformation the contribution of the second term in (14) has the same Borel exponent $e^{-m_h^2/M^2}$ as the lowest resonance contribution. The only difference is in pre-exponent factors: they are $1/M^2$ in front of the resonance term and Const. in front of non-diagonal terms. This difference was used in order to get rid of non-diagonal terms: application of the differential operator $(\partial/\partial(1/M^2)e^{m_h^2/M^2}$ to the sum rule kills the Borel non-suppressed nondiagonal terms, but deteriorates the accuracy and shrinks the applicability domain of the sum rule (particularly, the domain in x, where the sum rule is valid).

Show now that in the used here model of hadronic spectrum–resonance plus continuum, where continuum is given by the bare loop contribution, the second and third terms in (11) are in fact zero. Consider the bare loop represented by the diagram of Fig.3. For simplicity restrict ourselves by the case when all propagators are bosonic and all currents are scalar. (In the realistic case with quarks in internal lines conclusion will be the same). The imaginary part in s-channel of Fig.3 diagram is given by (quark masses are neglected):

$$Im\ T(p_1^2, p_2^2, q^2, s) = \int \ d^4k \frac{1}{(p_1 - k)^2(p_2 - k)^2}\delta\Big[(p_1 + q_1 - k)^2\Big]\delta(k^2) \tag{15}$$

Neglecting the higher twist terms $\sim p_{1,2}^2/q^2$ (15) is equal to (see [12], Appendix)

$$Im\ T(p_1^2, p_2^2, q^2, s) = \frac{\pi}{4\nu x} \int\limits_0^\infty \frac{1}{(u - p_1^2)(u - p_2^2)} \ du \tag{16}$$

where $\nu = qP$ and $x = -q^2/2\nu$. To derive (16) it is convenient to introduce

$$\begin{aligned} P &= (p_1 + p_2)/2 \\ r &= p_1 - p_2, \ r^2 = 0 \end{aligned} \tag{17}$$

and in the Lorenz system, where 4-vector P has only z-component and q - only time and z-components

$$r_0 \approx r_z \approx \frac{1}{2} \ \frac{p_1^2 - p_2^2}{\sqrt{-P^2}}, \quad r_\perp^2 = -\frac{1}{4} \ \frac{q^2(p_1^2 - p_2^2)^2}{\nu^2 - q^2P^2}, \tag{18}$$

$r_\perp^2$ is of higher twist and may be neglected. As follows from (16), in case of bare loop of Fig.3 the spectral function is proportional to $\delta(u_1 - u_2)$ and the contributions of areas II, III in Fig.1 are zero. Since one may expect, that more complicated diagrams are smaller and in any case their contributions in domains II, III are suppressed by Borel exponents, one may safely neglect them, as was done in (12).

3 Quark distributions in pion

It is enough to find the distribution of valence u-quark in π^+, since $\bar{d}(x) = u(x)$. The most suitable hadronic current in this case is the axial current

$$j_{\mu 5} = \bar{u}\gamma_\mu\gamma_5 d \tag{19}$$

In order to find the u-quark distribution, the electromagnetic current is chosen as u-quark current with the unit charge

$$j_\mu^{el} = \bar{u}\gamma_\mu u \tag{20}$$

The bare loop Fig.3 contribution is given by

$$Im\ \Pi_{\mu\nu\lambda\sigma} = -\frac{3}{(2\pi)^2}\ \frac{1}{2}\ \int\ \frac{d^4k}{k^2}\ \frac{1}{(k+p_2-p_1)^2}\delta[(q+k)^2]\delta[p_1-k)^2] \\ \times Tr\left\{\gamma_\lambda\hat{k}\gamma_\mu(\hat{k}+\hat{q})\gamma_\nu(\hat{k}+\hat{p}_2-\hat{p}_1)\gamma_\sigma(\hat{k}-\hat{p}_1)\right\} \tag{21}$$

The tensor structure, chosen to construct the sum rule is a structure proportional to $P_\mu P_\nu P_\lambda P_\sigma/\nu$. The reasons are the following. As is known, the results of the QCD sum rules calculations are more reliable, if invariant amplitude at kinematical structure with maximal dimension is used. Different $p_1 \neq p_2$ are important for us only in denominators, where they allow one to separate the terms in dispersion relations. In numerators one may restrict oneself to consideration of terms proportional to 4-vector P_μ and ignore the terms $\sim r_\mu$. Then the factor $P_\mu P_\nu$ provides the contribution of $F_2(x)$ structure function and the factor $P_\lambda P_\sigma$ corresponds to contribution of spin zero states. (The factor $1/\nu$ is scaling factor : $w_2 = F_2/\nu$.)

Let us use the notation

$$\Pi_{\mu\nu\lambda\sigma} = (P_\mu P_\nu P_\lambda P_\sigma/\nu)\Pi(p_1^2, p_2^2, x) + ... \tag{22}$$

Then $Im\Pi(p_1^2, p_2^2, x)$ can be calculated from (21) (eq.'s (15),(16) are exploited) and the result is [12]:

$$Im\Pi(p_1^2, p_2^2, x) = \frac{3}{\pi}x^2(1-x)\int\limits_0^\infty du_1 \int\limits_0^\infty du_2\ \frac{\delta(u_1-u_2)}{(u_1-p_1^2)(u_2-p_2^2)} \tag{23}$$

The matrix element of the axial current between vacuum and pion state is well known

$$\langle 0|j_{\mu 5}|\pi\rangle = ip_\mu f_\pi \tag{24}$$

where $f_\pi = 131MeV$. The use of (12), (23), (24) gives the sum rule for valence u-quark distribution in pion in the bare loop approximation [12]:

$$u_\pi(x) = \frac{3}{2\pi^2}\ \frac{M^2}{f_\pi^2} x(1-x)(1-e^{-s_0/M^2})e^{m_\pi^2/M^2}, \tag{25}$$

where s_0 is the continuum threshold. In ref.[12] the following corrections to (25) were accounted:

1. Leading order (LO) perturbative corrections, proportional to $ln(Q^2/\mu^2)$, where μ^2 is the normalization point. In what follows the normalization point will be chosen to be equal to the Borel parameter $\mu^2 = M^2$.

2. Power corrections - higher order terms of OPE. Among the latter, the dimension-4 correction, proportional to gluon condensate $\langle 0|\frac{\alpha_s}{\pi} G^n_{\mu\nu}\ G^n_{\mu\nu}|0\rangle$ was first accounted, but it was found that the gluon condensate contribution to the sum rule vanishes after double borelization. There are two types of vacuum expectation values (v.e.v) of dimension 6: one, where only gluonic fields enter:

$$\frac{g_s}{\pi}\alpha_s f^{abc}\langle 0|G^a_{\mu\nu}\ G^b_{\nu\lambda}\ G^c_{\lambda\mu}|0\rangle \tag{26}$$

and the other, proportional to four-quark operators

$$\langle 0|\bar\psi\Gamma\psi\cdot\bar\psi\Gamma\psi|0\rangle \tag{27}$$

It was shown in [12] that terms of the first type cancel in the sum rule and only terms of the second type survive. For the latter one may use the factorization hypothesis which reduces all the terms of this type to the square of quark condensate.

A remark is in order here. As was mentioneed in the Introduction, the present approach is invalid at small and large x. No-loop 4-quark condensate contributions, like Fig.4, are proportional to $\delta(1-x)$ and being outside of the applicability domain of the approach, cannot be accounted. In the same way, the diagrams, which can be considered as a radiative corrections to those, proportional to $\delta(1-x)$, must be also omitted.

All dimension-6 power corrections to the sum rule were calculated in ref.12 and the final result is given by (the pion mass is neglected):

$$\begin{aligned} xu_\pi(x) = \frac{3}{2\pi^2}\frac{M^2}{f_\pi^2}x^2(1-x)\Bigg[\Bigg(1+\left(\frac{a_s(M^2)\cdot ln(Q_0^2/M^2)}{3\pi}\right) \\ \times\left(\frac{1+4xln(1-x)}{x}-\frac{2(1-2x)lnx}{1-x}\right)\Bigg)\cdot(1-e^{-s_0/M^2}) \\ -\frac{4\pi\alpha_s(M^2)\cdot 4\pi\alpha_s a^2}{(2\pi)^4\cdot 3^7\cdot 2^6\cdot M^6}\cdot\frac{\omega(x)}{x^3(1-x)^3}\Bigg], \end{aligned} \tag{28}$$

where $\omega(x)$ is 4-order polynomial in x,

$$a = -(2\pi)^2\langle 0|\bar\psi\psi|0\rangle \tag{29}$$

$$\begin{aligned} \omega(x) = -5784x^4 - 1140x^3 - 20196x^2 \\ +20628x - 8292)ln(2) + 4740x^4 + 8847x^3 \\ + 2066x^2 - 2553x + 1416 \end{aligned} \tag{30}$$

$u_\pi(x)$ may be used as an initial condition at $Q^2 = Q_0^2$ for solution of QCD evolution equations (DGLAP) equations [1].

In numerical calculations we choose: the effective LO QCD parameter $\Lambda_{QCD}^{LO} = 200MeV$, $Q_0^2 = 2GeV^2$, $\alpha_s a^2(1GeV^2) = 0.13GeV^6$ [12]. The continuum threshold was varied in the interval $0.8 < s_0 < 1.2GeV^2$ and it was found, that the results only slightly depend on it. The analysis of the sum rule (28) shows, that it is fulfilled in the region $0.15 < x < 0.7$; the power corrections are less than 30% and the continuum contribution is small ($< 25\%$). The stability in the Borel mass parameter M^2 dependence in the region $0.4GeV^2 < M^2 < 0.6GeV^2$ is good. The result of our calculation of valence distribution in pion $xu_\pi(x, Q_0^2)$ is shown in Fig.5.

Suppose, that at small $x \lesssim 0.15$ $u_\pi(x) \sim 1/\sqrt{x}$ according to Regge behaviour and at large $x \gtrsim 0.7$ $u_\pi(x) \sim (1-x)^2$ according to quark counting rules. Then, matching these functions with (28), one may find the numerical values of the first and second moments of u-quark distribution

$$\mathcal{M}_1 = \int_0^1 u_\pi(x)dx \approx 0.84 \quad (0.85) \tag{31}$$

$$\mathcal{M}_2 = \int_0^1 xu_\pi(x)dx \approx 0.21 \quad (0.23) \tag{32}$$

(In the parenthesis we give the values, corresponding to $u_\pi(x) \sim 1 - x$ behaviour at large x.) The results only slightly depend on the points of matching (not more than 5%, when the lower matching point is varied in the region 0.15 - 0.2 and the upper one in the region 0.65 - 0.75). $\mathcal{M}_1$ has the meaning of the number of u-quarks in π^+ and should be $\mathcal{M} = 1$. The deviation of (31) from 1 characterizes the accuracy of our calculation. $\mathcal{M}_2$ has the meaning of the part of pion momentum carried by valence u-quark. Therefore, valence u and $\bar{d}$ quarks are carrying about 40% of the total momentum. In Fig.5 we plot also the valence u-quark distribution found in [6] by fitting the data on production of $\mu^+\mu^-$ and e^+e^- pairs in pion-nucleon collisions (Drell-Yan process). Comparing with the found here distribution it must be taken in mind, that the accuracy of our curve is of order of $10 - 20\%$, the last number refers to the border of the applicability domain. U-quark distribution found from the data on the Drell-Yan process is also not free from uncertainties. Particularly, what is measured in the Drell-Yan process is the quark fragmentation function into pion defined at $q^2 > 0$. In order to get quark distribution in pion defined at $q^2 < 0$, the procedure of analytical continuation is used, which may introduce some uncertainties, especially, at low normalization point, like $Q_0^2 = 2\ GeV^2$, to which the data in Fig.5 refer. For all these reasons we consider the agreement of two curves as good. The calculation of valence u-quark distribution in pion in the instanton model was done recently [14]. At intermediate x the values of $xu_\pi(x)$ found in [14], are about 20% higher, in comparison with ours. Recently also the pions valence quark momentum distribution using a Dyson-Schwinger equation model was found in [15]. Our results are in reasonable agreement with the results of [15].

[1] There was a misprint in the corresponding equation in [12] (eq.40 of [12]): instead of $\alpha_s(M^2)$ in the last term was $\alpha_s(Q_0^2)$. In numerical calculations the correct value $\alpha_s(M^2)$ was taken.

4 Quark distributions in ρ-meson

Let us calculate valence u-quarks distribution in ρ^+-meson (ρ – width is neglected). The choice of hadronic current is evident

$$j^\rho_\mu = \overline{u}\gamma_\mu d \tag{33}$$

The matrix element $\langle \rho^+ \mid j^\rho_\mu \mid 0\rangle$ is given by

$$\langle \rho^+ \mid j^\rho_\mu \mid 0\rangle = \frac{m^2_\rho}{g_\rho} e_\mu \tag{34}$$

where m_ρ is the ρ-meson mass, g_ρ is the $\rho-\gamma$ coupling constant, $g^2_\rho/4\pi = 1.27$, e_μ is the ρ-meson polarization vector. Consider the coordinate system, where the collision of ρ-meson with momentum p and virtual photon with momentum q proceeds along z-axes. The averaging over ρ polarizations is given by the formulae:
1. Longitudinally polarized ρ:

$$e^L_\mu e^L_\nu = \left(q_\mu - \frac{\nu p_\mu}{m^2_\rho}\right)\left(q_\nu - \frac{\nu p_\nu}{m^2_\rho}\right)\frac{m^2_\rho}{\nu^2 - q^2 m^2_\rho} \tag{35}$$

2. Transversally polarized ρ:

$$\sum_{T,r} e^r_\mu e^r_\nu = -\left(\delta_{\mu\nu} - \frac{p_\mu p_\nu}{m^2_\rho}\right) - \frac{m^2_\rho}{\nu^2 - q^2 m^2_\rho}\left(q_\mu - \frac{\nu p_\mu}{m^2_\rho}\right)\left(q_\nu - \frac{\nu p_\nu}{m^2_\rho}\right) \tag{36}$$

The imaginary part of the forward $\rho-\gamma$ scattering amplitude $W_{\mu\nu\lambda\sigma}$ (before multiplication by ρ-polarizations) satisfies the equations: $W_{\mu\nu\lambda\sigma}q_\mu = W_{\mu\nu\lambda\sigma}q_\nu = W_{\mu\nu\lambda\sigma}p_\lambda = W_{\mu\nu\lambda\sigma}p_\sigma = 0$, which follows from current conservation. (The indeces μ,ν refer to initial and final photon; λ,σ – to initial and final ρ.) The general form of $W_{\mu\nu\lambda\sigma}$ is:

$$\begin{aligned} W_{\mu\nu\lambda\sigma} = \Bigg[&\left(\delta_{\mu\nu} - \frac{q_\mu q_\nu}{q^2}\right)\left(\delta_{\lambda\sigma} - \frac{p_\lambda p_\sigma}{m^2_\rho}\right)A - \left(\delta_{\mu\nu} - \frac{q_\mu q_\nu}{q^2}\right)\left(q_\lambda - \frac{\nu p_\lambda}{m^2_\rho}\right)\left(q_\sigma - \frac{\nu p_\sigma}{m^2_\rho}\right)B \\ &-\left(p_\mu - \frac{\nu q_\mu}{q^2}\right)\left(p_\nu - \frac{\nu q_\nu}{q^2}\right)\left(\delta_{\lambda\sigma} - \frac{p_\lambda p_\sigma}{m^2_\rho}\right)C + \left(p_\mu - \frac{\nu q_\mu}{q^2}\right)\left(p_\nu - \frac{\nu q_\nu}{q^2}\right) \\ &\times\left(q_\lambda - \frac{\nu p_\lambda}{m^2_\rho}\right)\left(q_\sigma - \frac{\nu p_\sigma}{m^2_\rho}\right)D\Bigg] \end{aligned} \tag{37}$$

where A,B,C,D are invariant functions. Average (37) over polarizations for longitudinal and transverse ρ-mesons. We have

$$\begin{aligned} W_{\mu\nu\lambda\sigma}e^L_\lambda e^L_\sigma = &-\left(\delta_{\mu\nu} - \frac{q_\mu q_\nu}{q^2}\right)\left(A + \frac{\nu^2 - q^2 m^2_\rho}{m^2_\rho}B\right) + \\ &+\left(p_\mu - \nu\frac{q_\mu}{q^2}\right)\left(p_\nu - \nu\frac{q_\nu}{q^2}\right)\left(C + \frac{\nu^2 - q^2 m^2_\rho}{m^2_\rho}D\right) \end{aligned} \tag{38}$$

$$\frac{1}{2}\sum_{T,r} W_{\mu\nu\lambda\sigma} e^r_\lambda e^r_\sigma = -\left(\delta_{\mu\nu} - \frac{q_\mu q_\nu}{q^2}\right)A + \left(p_\mu - \frac{\nu q_\mu}{q^2}\right)\left(p_\nu - \frac{\nu q_\nu}{q^2}\right)C \tag{39}$$

From comparison of (37) and (38), (39) it is clear, that the proportional to $p_\mu p_\nu$ structure function $F_2(x)$ in the scaling limit ($\nu^2 \gg \mid q^2 \mid m_\rho^2$) is given by the contribution of invariants $C+(\nu^2/m_\rho^2)D$ in case of longitudinal and by invariant C in case of transversal ρ-mesons. This means, that in the forward scattering amplitude $W_{\mu\nu\lambda\sigma}$ (37) one must separate the structure proportional to $p_\mu p_\nu p_\lambda p_\sigma$ in the first case and the structure $\sim p_\mu p_\nu \delta_{\lambda\sigma}$ in the second case.

Consider now the non-forward 4-point correlator

$$\Pi_{\mu\nu\lambda\sigma}(p_1, p_2; q, q') = -i \int d^4x d^4y d^4z e^{ip_1 x + iqy - ip_2 z}$$

$$\times \langle 0 \mid T\ \{j^\rho_\lambda(x),\ j^{el}_\mu(y),\ j^{el}_\nu(0),\ j^\rho_\sigma(z)\} \mid 0\rangle, \tag{40}$$

where the currents $j^{el}_\mu(x)$ and $j^\rho_\lambda(x)$ are given by (20) and (33). It is evident from the said above, that in the non-forward amplitude for determination of u-quark distribution in longitudinal ρ-meson the most suitable tensor structure is that, proportional to $P_\mu P_\nu P_\sigma P_\lambda$, while u-quark distribution in transverse ρ can be found by considering the invariant function at the structure $-P_\mu P_\nu \delta_{\lambda\sigma}$ (P is given by (17)).

Calculate first the bare loop contribution (diagram of Fig.3). In case of longitudinal ρ-meson the tensor structure, which is separated is the same, as in the case of pion. Since at $m_q = 0$ bare loop contributions for vector and axial hadronic currents are equal, the only difference from the pion case is in the normalization. It can be shown, that u-quark distribution in longitudinal ρ-meson can be found from (25) by substitutions $m_\pi \to m_\rho$, $f_\pi \to m_\rho/g_\rho$ and therefore

$$u^L_\rho = \frac{3}{2\pi^2}\frac{M^2}{m^2_\rho} g^2_\rho x(1-x) e^{m^2_\rho/M^2}(1 - e^{-s_0/M^2}) \tag{41}$$

The calculation of g^2_ρ performed in the same approximation in [16] leads to

$$\frac{g^2_\rho M^2}{m^2_\rho 4\pi}(1 - e^{-s_0/M^2}) e^{m^2_\rho/M^2} = \pi \tag{42}$$

(the definition of g_ρ used here differs from that in [16] by a factor $1/\sqrt{2}$). The substitution of (42) in (41) gives

$$u^L_\rho(x) = 6x(1-x) \tag{43}$$

and we have

$$\int\limits_0^1 u^L_\rho(x)dx = 1, \tag{44}$$

as it should be. Also,

$$\int\limits_0^1 x u^L_\rho(x)dx = \frac{1}{2}, \tag{45}$$

is in correspondence with naive quark model, where u-quarks are carrying one half of total momentum. The calculation of the term, proportional to the structure $P_\mu P_\nu \delta_{\lambda\sigma}$ in the diagram of Fig.3 gives

$$Im\Pi^{(0)}_{\mu\nu\lambda\sigma} \equiv -\frac{1}{\nu} P_\mu P_\nu \delta_{\lambda\sigma} Im\Pi^{(0)}_T = -\frac{3}{2\pi}\frac{1}{\nu} P_\mu P_\nu \delta_{\lambda\sigma} x\left[\frac{1}{2} - x(1-x)\right] \int \frac{udu}{(u-p_1^2)(u-p_2^2)} \quad (46)$$

After borelization we get for u-quark distribution in transversally polarized ρ-meson in bare loop approximation

$$u^T_\rho(x) = \frac{3}{(2\pi)^2} g_\rho^2 \frac{M^4}{m_\rho^4} e^{m_\rho^2/M^2} E_1\left(\frac{s_0}{M^2}\right)\left[\frac{1}{2} - x(1-x)\right] \quad (47)$$

where

$$E_1(z) = 1 - (1+z)e^{-z} \quad (48)$$

Let us use (42), put $M^2 = m_\rho^2$ and neglect the terms $\sim e^{-s_0/m_\rho^2}$. Then a simple formula for $u^T_\rho(x)$ follows:

$$u^T_\rho(x) = 3\left[\frac{1}{2} - x(1-x)\right] \quad (49)$$

U-quark distribution (49) has the expected properties:

$$\int_0^1 u^T_\rho(x)dx = 1 \quad (50)$$

$$\int_0^1 x u^T_\rho(x)dx = \frac{1}{2} \quad (51)$$

Take in account LO perturbative correction, proportinal to $ln\ Q^2/\mu^2$ and choose $Q^2 = Q_0^2$ for the point where we calculate our sum rules. The result is (the second term in square brackets corresponds to the perturbative correction):

$$u^L_\rho(x) = \frac{3M^2}{4\pi^2}\frac{g_\rho^2}{m_\rho^2} e^{m_\rho^2/M^2} x(1-x)\left[1 + \frac{a_s(\mu^2) ln(Q_0^2/\mu^2)}{3\pi}\right.$$
$$\left.\times\left(1/x + 4ln(1-x) - \frac{2(1-2x)ln\ x}{1-x}\right)\right](1 - e^{-s_0/M^2}) \quad (52)$$

and

$$u^T(x) = \frac{3}{8\pi^2}\frac{g_\rho^2}{m_\rho^4} e^{m_\rho^2/M^2} \cdot M^4 \cdot E_1\left(\frac{s_0}{M^2}\right) \cdot \varphi_0(x)$$

$$\left[1 + \frac{ln(Q_0^2/\mu^2)\cdot\alpha_s(\mu^2)}{3\pi} \cdot \left((4x-1)/\varphi_0(x) + 4ln(1-x) - \frac{2(1-2x+4x^2)lnx}{\varphi_0(x)}\right)\right] \quad (53)$$

where

$$\varphi_0(x) = 1 - 2x(1-x) \tag{54}$$

Turn now to consideration of power correction contribution to the sum rules. The power correction of lower dimension is proportional to the gluon condensate $\langle G^q_{\mu\nu} G^q_{\mu\nu}\rangle$ with $d = 4$. As was discussed above, only s-shannel diagrams (Fig.1) exist in the case of double borelization. The $\langle G^q_{\mu\nu} G^q_{\mu\nu}\rangle$ correction was calculated in a standard way in the Fock-Schwinger gauge $x_\mu A_\mu = 0$ [17].

The quark propagator $iS(x,y) = \langle\psi(x)\psi(y)\rangle$ in the external field A_μ has the well-known form [13, 9, 18]. In the π-meson case the sum of all diagrams, corresponding to $\langle G^a_{\mu\nu} G^a_{\mu\nu}\rangle$ corrections (Fig.6), was found to be zero after double borelization [12]. For ρ-meson, however, $\langle G^a_{\mu\nu} G^a_{\mu\nu}\rangle$ correction are equal to zero for longitudinally polarized ρ (ρ_L) but are not vanishing for transversally polarized $\rho(\rho_T)$

$$Im\Pi_T^{(d=4)} = -\frac{\pi}{8x}\langle 0 \mid \frac{\alpha_s}{\pi} G^2_{\mu\nu} \mid 0\rangle \tag{55}$$

All diagrams here and in what follows are calculated using a program for analytical calculations REDUCE. Before we discuss $d = 6$ contribution, let us remind, that we should not take into account non-loop diagrams and diagrams, which can be treated as their evolution (for example see Fig.7). There is a large number of loop diagrams for $d = 6$ correction. It is convenient to divide them into two types and discuss these types separately:
Type I-diagrams where only interaction with the external gluon field is taken into account – see Fig.8,9.
Type II – diagrams, where expansion of quark field is also accounted (∇-covariant derivate)

$$\psi(x) = \psi(0) + x_{\alpha_1}\ [\nabla_{\alpha_1}\psi(0)] + \frac{1}{2} x_{\alpha_1} x_{\alpha_2}\ [\nabla_{\alpha_1}\nabla_{\alpha_2}\psi(0)] + ... \tag{56}$$

The examples of such diagrams are shown in Fig.10,11. Discuss briefly the special features of calculation of this two types of diagrams. The diagram of type I (Fig.8) are, obviously, proportional to $\langle 0 \mid g^3 f^{abc} G^a_{\mu\nu} G^b_{\alpha\beta} G^c_{\rho\sigma} \mid 0\rangle$ and when calculating it is convenient to use the representation of this tensor structure suggested in [19]

$$\langle 0 \mid g^3 f^{abc} G^a_{\mu\nu} G^b_{\alpha\beta} G^c_{\rho\sigma} \mid 0\rangle = 1/24 \langle 0 \mid g^3 f^{abc} G^a_{\gamma\delta} G^b_{\delta\epsilon} G^c_{\epsilon\gamma} \mid 0\rangle \tag{57}$$

$$\times (g_{\mu\sigma} g_{\alpha\nu} g_{\beta\rho} + g_{\mu\beta} g_{\alpha\rho} g_{\sigma\nu} + g_{\alpha\sigma} g_{\mu\rho} g_{\nu\beta} + g_{\rho\nu} g_{\mu\alpha} g_{\beta\sigma}$$

$$- g_{\mu\beta} g_{\alpha\sigma} g_{\rho\nu} - g_{\mu\sigma} g_{\nu\beta} g_{\alpha\rho} - g_{\alpha\nu} g_{\mu\rho} g_{\beta\sigma} - g_{\beta\rho} g_{\mu\alpha} g_{\nu\sigma})$$

The diagrams of Fig.9 are proportional to $\langle 0 \mid D_\rho G^a_{\mu\nu} D_\tau G^a_{\alpha\beta} \mid 0\rangle$ and $\langle 0 \mid G^a_{\mu\nu} D_\rho D_\tau G^a_{\alpha\beta} \mid 0\rangle$. Using the equation of motion it was found in [19] that[2]

$$-\langle 0 \mid D_\rho G^a_{\mu\nu} D_\sigma G^a_{\alpha\beta} \mid 0\rangle = \langle 0 \mid G^a_{\mu\nu} D_\rho D_\sigma G^a_{\alpha\beta} \mid 0\rangle = 2O^-\ [g_{\rho\sigma}(g_{\mu\beta} g_{\alpha\nu} - g_{\mu\alpha} g_{\nu\beta})$$

[2]Note that our choice of sign of g is opposite to those of [19].

$$+\frac{1}{2}(g_{\mu\beta}g_{\alpha\sigma}g_{\rho\nu}+g_{\alpha\nu}g_{\mu\rho}g_{\beta\sigma}-g_{\alpha\sigma}g_{\mu\rho}g_{\nu\beta}-g_{\rho\nu}g_{\mu\alpha}g_{\beta\sigma})]$$

$$+O^{+}(g_{\mu\sigma}g_{\alpha\nu}g_{\beta\rho}+g_{\mu\beta}g_{\alpha\rho}g_{\sigma\nu}-g_{\mu\sigma}g_{\alpha\rho}g_{\nu\beta}-g_{\rho\beta}g_{\mu\alpha}g_{\nu\sigma}),$$

$$O^{\pm}=\frac{1}{72}\langle 0\mid g^2 j^a_\mu j^a_\mu\mid 0\rangle \mp \frac{1}{48}\langle 0\mid g f^{abc}G^a_{\mu\nu}G^b_{\nu\lambda}G^c_{\lambda\mu}\mid 0\rangle, \tag{58}$$

where $j^a_\mu=\sum\bar\psi_i\gamma_\mu(\lambda^a/2)\psi_i$.

From (57) and (58) one may note that these tensor structures are proportional to two vacuum averages:

$$\langle 0\mid g^2 j^2_\mu\mid 0\rangle \quad\text{and}\quad \langle 0\mid g^3 G^a_{\mu\nu}G^b_{\nu\rho}G^c_{\rho\mu}f^{abc}\mid 0\rangle.$$

The first of these, $\langle 0\mid g^2 j^2_\mu\mid 0\rangle$, by use of the factorization hypothesis easily reduces to $\langle g\bar\psi\psi\rangle^2$ which is well known,

$$\langle 0\mid g^2 j^2_\mu\mid 0\rangle=-(4/3)[\langle 0\mid g\bar\psi\psi\mid 0\rangle]^2. \tag{59}$$

But $\langle 0\mid g^3 G^a_{\mu\nu}G^b_{\nu\rho}G^c_{\rho\mu}f^{abc}\mid 0\rangle$ is not well known; there are only some estimates based on the instanton model [20, 21]. In the π-meson case the terms, proportional to $\langle 0\mid g^3 f^{abc}G^a_{\mu\nu}G^b_{\nu\rho}\,G^c_{\rho\mu}\mid 0\rangle$ exactly cancelled [12]. The similar cancellation takes place for ρ_L. But there is no such cancellation for ρ_T and one should estimate $\langle 0\mid g^3 f^{abc}G^a_{\mu\nu}G^b_{\nu\rho}G^c_{\rho\mu}\mid 0\rangle$. The estimation, based on the instanton model [20], gives

$$-\langle g^3 f^{abc}G^a_{\mu\nu}G^b_{\nu\rho}G^c_{\rho\mu}\rangle=\frac{48\pi^2}{5}\frac{1}{\rho_c^2}\langle 0\mid(\alpha_s/\pi)G^2_{\mu\nu}\mid 0\rangle, \tag{60}$$

where ρ_c is the effective instanton radius.

Among the diagrams of type II (Figs.10,11) only those, where the interaction with the vacuum takes place inside the loop, are considered. Such diagrams cannot be treated as the evolution of any non-loop diagrams and are pure power corrections of dimension 6. All these diagrams are, obviously, proportional to

$$\langle 0\mid\bar\psi^d_\alpha\psi^b_\beta D_\rho G^n_{\mu\nu}\mid 0\rangle,\quad \langle 0\mid\bar\psi^d_\alpha(\nabla_\tau\psi^b_\beta)G^n_{\mu\nu}\mid 0\rangle,\quad \langle 0\mid(\nabla_\tau\bar\psi^d_\alpha)\psi^b_\beta G^n_{\mu\nu}\mid 0\rangle.$$

These tensor structure were considered in [13] where with the help of equation of motion the following results were obtained[3]:

$$\langle 0\mid\bar\psi^d_\alpha\psi^b_\beta(D_\sigma G_{\mu\nu})^n\mid 0\rangle=\frac{g\langle 0\mid\bar\psi\psi\mid 0\rangle^2}{3^3\cdot 2^5}(g_{\sigma\nu}\gamma_\mu-g_{\sigma\mu}\gamma_\nu)_{\beta\alpha}(\lambda^n)^{bd}, \tag{61}$$

$$\langle 0\mid\bar\psi^d_\alpha(\nabla_\sigma\psi_\beta)^b G^n_{\mu\nu}\mid 0\rangle=\frac{g\langle 0\mid\bar\psi\psi\mid 0\rangle^2}{3^3\cdot 2^6}[g_{\sigma\mu}\gamma_\nu-g_{\sigma\nu}\gamma_\mu-i\varepsilon_{\sigma\mu\nu\lambda}\gamma_5\gamma_\lambda]_{\beta\alpha}(\lambda^n)^{bd}. \tag{62}$$

The term $\langle 0\mid(\nabla_\sigma\bar\psi_\alpha)^d\bar\psi^b_\beta G^n_{\mu\nu}\mid 0\rangle$ can easily be calculated using (61),(62)

[3]The sign errors in front of g in eq.'s (23),(24),(A1),(A2) of [13] are corrected.

$$\langle 0 \mid (\nabla_\sigma \bar{\psi}_\alpha)^d \bar{\psi}^b_\beta G^n_{\mu\nu} \mid 0\rangle = \frac{g\langle 0 \mid \bar{\psi}\psi \mid 0\rangle^2}{3^3 \cdot 2^6}$$

$$\times \left[g_{\sigma\mu}\gamma_\nu - g_{\sigma\nu}\gamma_\mu + i\varepsilon_{\sigma\mu\nu\lambda}\gamma_5\gamma_\lambda\right]_{\beta\alpha}(\lambda^n)^{bd}. \quad (63)$$

For diagrams in Fig.11 we use the following expansion of the gluon propagator:

$$S^{np}_{\nu\rho}(x-y,y) = \frac{-i}{(2\pi)^4} g f^{npl} \int \frac{d^4k}{k^4} e^{-ik(x-y)} \cdot \left\{ \left[-ik_\lambda y_\alpha G^l_{\alpha\lambda} - \frac{2}{3} i (y_\alpha y_\beta k_\lambda \right.\right.$$

$$\left. - \frac{iy_\beta}{k^2}(k^2\delta_{\alpha\lambda} - 2k_\alpha k_\lambda))(D_\alpha G_{\beta\lambda})^l + \frac{1}{3}\left(y_\alpha + \frac{2ik_\alpha}{k^2}\right)\right.$$

$$\left.\left. \times (D_\lambda G_{\alpha\lambda})^l \right] \delta_{\nu\rho} + 2\left[G^l_{\nu\rho} + 2i\frac{k_\alpha}{k^2}(D_\alpha G_{\nu\rho})^l \right] \right\} \quad (64)$$

This expression can be found by the method of the calculation of the gluon propagator in the external vacuum gluon field suggested in [17] (see also [18, 22]). The total number of $d = 6$ diagrams is enormous – about 500. Collecting the results together we get finally the following sum rules for u^L_ρ

$$x u^L_\rho(x) = \frac{3}{4\pi^2} M^2 \frac{g^2_\rho}{m^2_\rho} e^{m^2_\rho/M^2} x^2(1-x)\left[\left(1 + \left(\frac{a_s(M^2)\cdot ln(Q^2_0/M^2)}{3\pi} \right) \right.\right.$$

$$\left.\left. \times \left(\frac{1 + 4xln(1-x)}{x} - \frac{2(1-2x)lnx}{1-x} \right) \right)(1 - e^{-s_0/M^2}) - \frac{\alpha_s(M^2)\cdot\alpha_s a^2}{\pi^2\cdot 3^7\cdot 2^6\cdot M^6} \cdot \frac{\omega(x)}{x^3(1-x)^3} \right], \quad (65)$$

where a and $\omega(x)$ are given by (29), (30). A remark here is in order. In (65) (as well in (28)) the strong coupling constant g_s is generated in the diagrams in two ways:
1) due to explicit quark-gluon interaction (vertices of a hard gluon line in the diagrams in Figs.10 and 11, or vertices of external gluon in the diagrams in Figs.8 and 9), and it is reasonable to take it at the renormalization point $\mu^2 = M^2$; 2) due to the equation of motion, and its normalization point should be taken in such a way that the quantity $\alpha_s\langle 0 \mid \bar{\psi}\psi \mid 0\rangle^2$ is a renormalization group invariant. The notations in (28),(65) reflect this fact.

Sum rules for $u^L_\rho(x)$ are fullfilled in wide region of x: $0.1 < x < 0.85$. Borel mass M^2 dependence of $xu^L_\rho(x)$ at various x is plotted in Fig.12. One can see that it is weak in the whole range of x, except $x \le 0.1$ and $x \ge 0.75$. As discussed in the Introduction the reason of a more strong M^2-dependence at small and large x is connected with the fact, that our approach is invalid at small x and x, close to 1. It is manifested by the blow up of dimension 6 correction at $x \to 0$ and $x \to 1$ in eq.(65). So, the applicability domain of the sum rule can be found from the sum rule itself. Fig.13 presents $xu^L_\rho(x)$ as a function of x. $M^2 = 1$ GeV^2 and $s_0 = 1.5$ GeV^2, $Q^2_0 = 4$ GeV^2 were chosen, the other set of parameters – Λ^{LO}_{QCD} and $\alpha_s a^2$ is the same as in the calculation of $xu_\pi(x)$.

Valence u-quark distribution in transversally polarized ρ-meson is given by

$$x u^T_\rho(x) = \frac{3}{8\pi^2} g^2_\rho e^{m^2_\rho/M^2} \frac{M^4}{m^4_\rho} x \left\{ \varphi_0(x) E_1\left(\frac{s_0}{M^2}\right)\left[1 + \frac{1}{3\pi} ln\left(\frac{Q^2_0}{M^2}\right)\alpha_s(M^2)\left(\frac{(4x-1)}{\varphi_0(x)} + \right.\right.\right.$$

$$+4ln(1-x)-\frac{2(1-2x+4x^2)lnx}{\varphi_0(x)}\Bigg)\Bigg]-\frac{\pi^2}{6}\ \frac{\langle 0|(\alpha_s/\pi)G^2|0\rangle}{M^4x^2}$$

$$+\frac{1}{2^8\cdot 3^5M^6x^3(1-x)^3}\langle 0|g^3f^{abc}G^a_{\mu\nu}G^b_{\nu\lambda}G^c_{\lambda\mu}|0\rangle\xi(x)$$

$$+\frac{\alpha_s(M^2)(\alpha_s a^2)}{2^5\cdot 3^8\pi^2M^6x^3(1-x)^3}\chi(x)\Bigg\} \tag{66}$$

$$\xi(x)=-1639+8039x-15233x^2+10055x^3-624x^4-974x^5 \tag{67}$$

$$\chi(x)=8513-41692x+64589x^2-60154x^3+99948x^4$$
$$-112516x^5+45792x^6+(-180-8604x+53532x^2$$
$$-75492x^3-28872x^4+109296x^5-55440x^6)ln2 \tag{68}$$

The standard value [16] of gluonic condensate $\langle 0\mid(\alpha_s/\pi)G^2\mid 0\rangle=0.012\ GeV^4$ was taken in numerical calculations. Unlike the cases of $u_\pi(x)$ and $u^L_\rho(x)$, dimension-6 power correction, proportional to $\langle 0|gf^{abc}G^a_{\mu\nu}G^b_{\nu\lambda}G^c_{\lambda\mu}\mid 0\rangle$, is not cancelled here. Its contribution is calculated with the help of the instanton gas model – eq.(60). The effective instanton radius ρ_c was chosen as $\rho_c=0.5fm$. This value is between the estimations of [20] ($\rho_c=1fm$) and [21] ($\rho_c=0.33fm$). (In the recent paper [23] the arguments were presented that the liquid gas instanton model overestimates higher order gluonic condensates and in order to correct this effect larger values of ρ_c comparing with [21] should be used). Borel mass dependence of $xu_T(x)$ is shown in Fig.14. As is seen from Fig.14, in the interval $0.2<x<0.65$ the M^2-dependence is weak at $0.8<M^2<1.2\ GeV^2$. Fig.15 shows $xu_T(x)$ at $M^2=1\ GeV^2$ and $Q_0^2=4\ GeV^2$. Dashed lines demonstrate the influence of the variation of ρ_c in the final result: the lower line corresponds to $\rho_c=0.6fm$ and the upper – to $\rho_c=0.4fm$. Our results are reliable at $0.2<x<0.65$, where $d=4$ and $d=6$ (separately) power corrections comprise less than 30% of the bare loop contribution. ($\langle 0|(\alpha_s/\pi)G^2|0\rangle$ and $\langle 0|g^3f^{abc}G^a_{\mu\nu}G^b_{\nu\lambda}G^c_{\lambda\mu}|0\rangle$ contributions are of the opposite sign and compensate one another, $\alpha_s(M^2)\alpha_s a^2$ contribution is negligible.) At $\rho_c=0.4fm$ the applicability domain shrinks to $0.25<x<0.6$. The moments of quark distributions in longitudinal ρ-meson are calculated in the same way, as it was done in the case of pion: by matching with Regge behaviour $u(x)\sim 1/\sqrt{x}$ at low x and with quark counting rule $u(x)\sim(1-x)^2$ at large x. The matching points were chosen as $x=0.10$ at low x and $x=0.80$ at large x. The numerical values of moments for longitudinally polarized ρ are

$$\mathcal{M}^L_1=\int\limits_0^1 dxu^L_\rho(x)=1.06\quad(1.05)$$

$$\mathcal{M}^L_2=\int\limits_0^1 xdxu^L_\rho(x)=0.39\quad(0.37) \tag{69}$$

The values of momenta, obtained by assuming that $u(x)\sim(1-x)$ at large x are given in the parenthesis.

Reliable calculation of moments in the case of transversally polarized ρ-meson is impossible, because of a narrow applicability domain in x and the form of u-quark distribution – Fig.15, which does not allow soft matching with expected behaviour $xu_\rho^T(x)$ at small and large x.

The comparison of u-quark distributions in longitudinally and transversally polarized ρ-mesons shows a strong difference of them: the curvatures have the opposite sign: $u_\rho^L(x)$ has a maximum at intermediate $x \sim 0.5$ while $u_\rho^T(x)$ has a minimum there. Strongly different are also the second moments in pion and in longitudinal ρ-meson: the total part of the momentum, carried by valence quarks and antiquarks $-(u + \bar{d})$ in longitudinal ρ-meson is about 0.8, while in pion it is much less – about 0.4-0.5. The same amount as in pion one may expect in transverse ρ (Fig.15), nevertheless, that it is impossible to calculate a precise number. Therefore, pion and transverse ρ-mesons in this aspect behave like a nucleon, where about 50% of total momentum is carried by gluons and sea quarks. In longitudinal ρ the situation is different – only about 20% of momentum is left for gluons and sea quarks. It must be mentioned, that in case of transverse ρ the accuracy of our results are worse than for longitudinal ρ, because the contribution of higher order terms of OPE is larger and the applicability domain in x is narrower. This fact, however, does not change the qualitative conclusion formulated above. Now let us discuss the nonpolarizied ρ-meson case. Quark distribution function $u(x)$ in this case is equal to:

$$u_\rho(x) = (u_\rho^L(x) + 2u_\rho^T(x))/3$$

and we can determine $u(x)$ only in the region, where sum rules for $u_\rho^L(x)$ and u_ρ^T are fulfiled, i.e. $0.2 \lesssim x \leq 0.65$. In this region $u_\rho(x)$ is found to be very close to $u_\pi(x)$ (the difference in whole range of x is not more than 10-15%).

5 Summary and discussion

Let us first discuss the accuracy of our results. In case of u-quark distribution in pion the main uncertainty comes from the magnitude of $\alpha_s\langle 0 \mid \bar{\psi}\psi \mid 0\rangle^2$. For renorminvariant quantity $(2\pi)^4\alpha_s\langle \mid \bar{\psi}\psi \mid 0\rangle^2$ in our calculations we took the value 0.13 Gev^6. In fact, however, it is uncertain by a factor of 2. (Recent determination [24] of this quantity from τ-decay data indicates that it may be two times larger). Also the perturbative corrections introduce some uncertainties, especially at large $x, (x > 0.6)$ where the accounted LO correction is large. (E.g. instead of $\Lambda_{QCD} = 200$ MeV the value $\Lambda_{QCD} = 250$ MeV could be taken). The estimation of both effects shows, that they may result in 10-15% variation of $xu_\pi(x)$ – increasing at $x < 0.3$ and decreasing at $x > 0.3$. One should note, that our estimation of the second moment of quark distribution in π-meson (32) differ from those obtained in [25]. The origin of this discrepancy is not completely clear now: partly it could be related with the difference of the value of parameters used in [25] ($\Lambda_{QCD}^{LO} = 100MeV,\ Q_0^2 = 1GeV^2$) from our choise of parameters, and partly, maybe, with the uncertainty of our estimations of the moments.

In case of u-quark distribution in longitudinally polarized ρ-meson the uncertainties in $\alpha_s\langle 0 \mid \bar{\psi}\psi \mid 0\rangle^2$ do not play any role, because of higher values of M^2 and the main source of them is the perturbative corrections. They influence only high x domain, $x > 0.5$.

The accuracy of our results for u-quark distribution in transversally polarized ρ-meson is worse, because of a large role of $d = 4$ and $d = 6$ gluonic condensate contributions. The variation of $xu_\rho^T(x)$ arising from uncertainties of $d = 6$ gluonic condensates was shown in Fig.15. The gluonic condensate $\langle 0 \mid (\alpha_s/\pi)G^2 \mid 0\rangle$ is also uncertain by a factor 1.5. It may result in 30-40% variation of xu_ρ^T at $x \approx 0.3 - 0.4$, but much less at $x \approx 0.5 - 0.6$. At least, these uncertainties do not influence the shape of u-quark distribution. (The LO perturbative corrections are no more than 20% at small x and negligible at large x).

Fig.16 gives the comparison of valence u-quark distributions in pion, longitudinally and transversally polarized ρ-mesons. The shapes of curves are quite different, especially of $xu_\rho^T(x)$ in comparison with $xu_\rho^L(x)$ and $xu_\pi(x)$. Any uncertainties in our calculations cannot influence this basic conclusion. The values of moments of quark distributions are also different – see the discussion at the end of Sec.4.

The main physical conclusion is: the quark distributions in pion and ρ-meson have not to much in common. The specific properties of pion, as a Goldstone boson manifest themselves in different quark distributions in comparison with ρ. $SU(6)$ symmetry, probably, may take place for static properties of π and ρ, but not for their internal structure. This fact is not surprising. Quark distributions have sense in fastly moving hadrons. However, $SU(6)$ symmetry cannot be selfconsistently generalized to relativistic case [26]. We have no explanation, why u-quark distributions in pion and nonpolarized ρ-meson at $0.2 < x < 0.65$ are close to one another – is it a pure accident or there are some deep reasons for it.

Acknowledgements

The research described in this publication was made possible in part by Award No RP2-2247 of U.S. Civilian Research and Development Foundation for Independent States of Former Soviet Union (CRDF) and by Russian Found of Basic Research grant 00-02-17808.

References

[1] A.M. Cooper-Sarkar, R.C.E. Davenish and A.De Roeck, Int. Journ. Mod. Phys. A **13**, 3385 (1998).

[2] H.L.Lai, et al. (CTEQ Collaboration) Eur. Phys. J. C **12**, 375 (2000).

[3] A.D. Martin, R.G. Roberts, W.J. Stirling, R.S. Thorne Eur. Phys. J. C **4**, 463 (1998).

[4] M. Glück, E. Reya and A. Vogt, Eur. Phys. J. C **5**, 461 (1998).

[5] P. Aurenche et al, Phys. Lett. B **333**, 517 (1989).

[6] M. Glück, E. Reya and A. Vogt, Z. Phys. C **53**, 651 (1992).

[7] P.J. Sutton, A.D. Martin, B.G. Roberts and W.J. Stirling, Phys. Rev. D **45** 2349 (1992).

[8] B.L. Ioffe, JETP Lett. **42**, 327 (1985).

[9] V.M. Belyaev and B.L. Ioffe, Nucl. Phys. B **310**, 548 (1988).

[10] A.S. Gorsky, B.L. Ioffe, A.Yu. Khodjamirian and A.G. Oganesian, Z. Phys. C **44**, 523 (1989).

[11] B.L. Ioffe and A.Yu. Khodjamirian, Phys. Rev. D **51** 3373 (1995).

[12] B.L. Ioffe and A.G. Oganesian, Eur. Phys. J. C **13**, 485 (2000).

[13] B.L. Ioffe and A.V. Smilga, Nucl. Phys. B **216**, 373 (1983).

[14] A.E. Dorokhov and L. Tomio, Phys. Rev. D **62**, 014016 (2000).

[15] M.B. Hecht, C.D. Roberts and S.M. Schmidt, hep-ph/0008049.

[16] M.A. Shifman, A.I. Vainshtein and V.I. Zakharov, Nucl. Phys. B **147**, 448 (1979).

[17] A.V. Smilga, Sov. J. Nucl. Phys. **35**, 271 (1982).

[18] V.A. Novikov, M.A. Shifman, A.I. Vainshtein and V.I. Zakharov, Fortschr. Phys. **32**, 585 (1984).

[19] S.N. Nikolaev and A.V. Radyushkin, Nucl. Phys. B **213**, 189 (1983).

[20] V.A. Novikov, M.A. Shifman, A.I. Vainshtein and V.I. Zakharov, Phys. Lett. B **86**, 347 (1979).

[21] T. Schäfer and E.V. Shuryak, Rev. Mod. Phys. **70**, 323 (1998).

[22] J. Govaerts, F. de Viron, D. Gusbin, J. Weyers, Nucl. Phys. B **248**, 1 (1984).

[23] B.L. Ioffe and A.V. Samsonov, Phys. At. Nucl. **63**, 1448 (2000).

[24] B.L. Ioffe and K.N. Zyablyuk, hep-ph/0010089.

[25] V.M. Belyaev and B.Yu. Block, Yad.Fiz. **43**, 706 (1986).

[26] B.V. Geshkenbein, B.L. Ioffe, M.S. Marinov and V.I. Roginsky, Phys.Lett. **16**, 347 (1965).

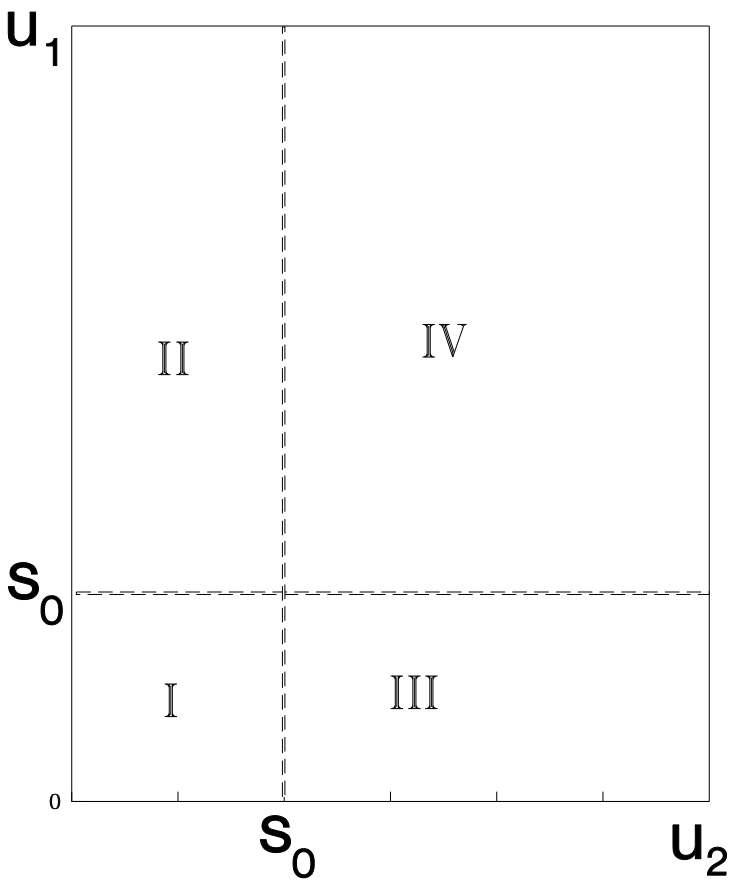

Figure 1: Integration region in the double dispersion representation.

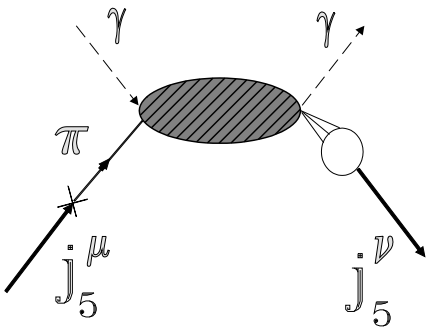

Figure 2: Example of the non-diagonal transition

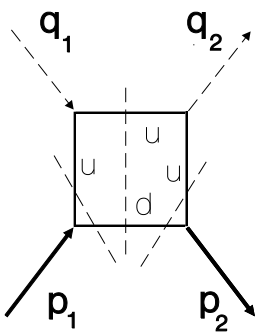

Figure 3: Diagram, corresponding to the unit operator contribution. Dashed lines with arrows correspond to the photon, thick solid - to hadron current

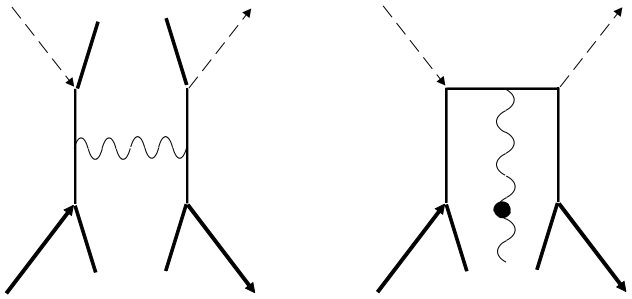

Figure 4: Examples of the non-loop diagrams of dimension 4. Wave lines correspond to gluons, dot means derivative, other notations as in Fig.3.

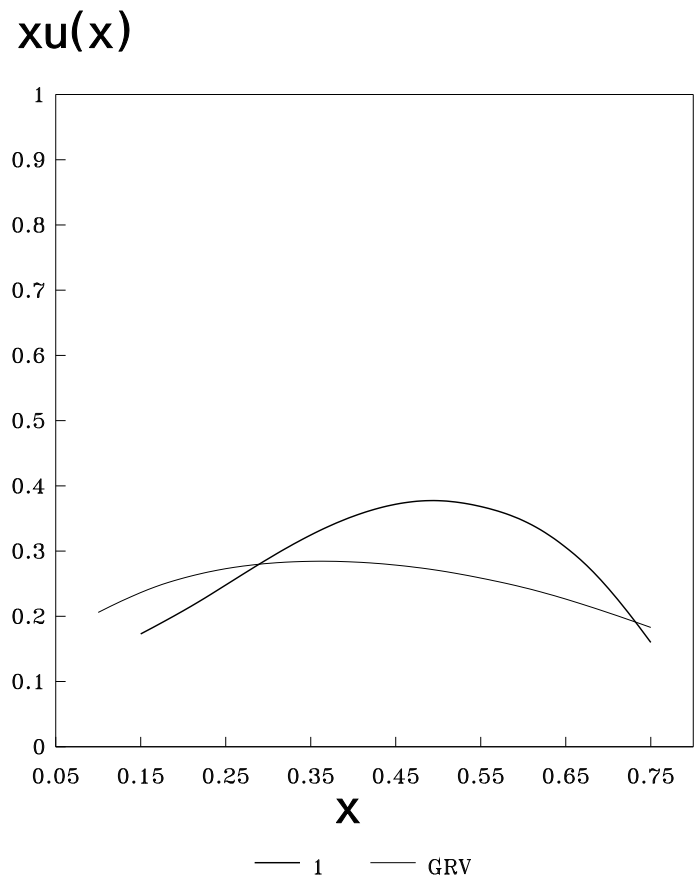

Figure 5: Quark distribution function in pion, noted "1". For comparison the fit from [6], labelled "GRV", is shown.

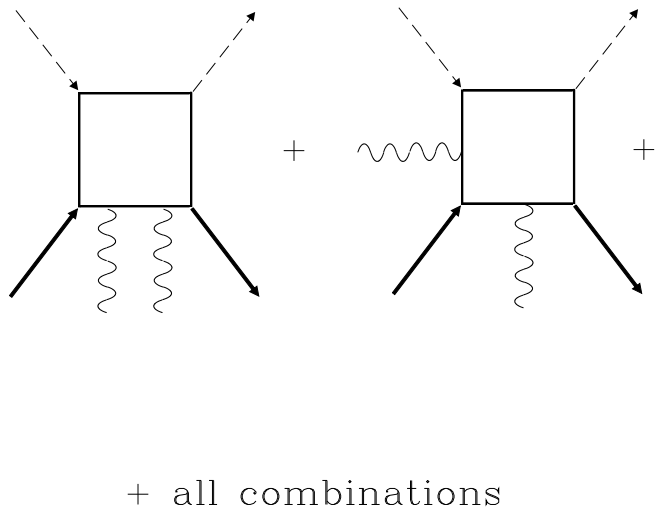

Figure 6: Diagrams, corresponding to the $d = 4$ operator contribution. Dashed lines with arrows correspond to the photon, thick solid - to the hadron current, wave lines correspond to the external gluon field

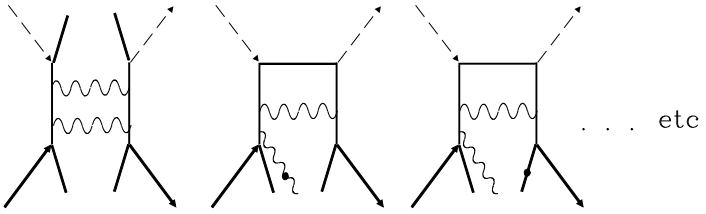

Figure 7: Dimension 6 diagrams corresponding to evolution of non-loop diagrams. All notations as in Fig.4

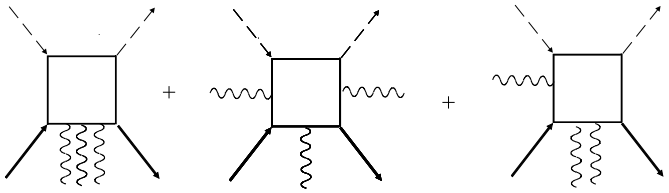

Figure 8: Diagrams of dimension 6, see text. All notations as in Fig.4

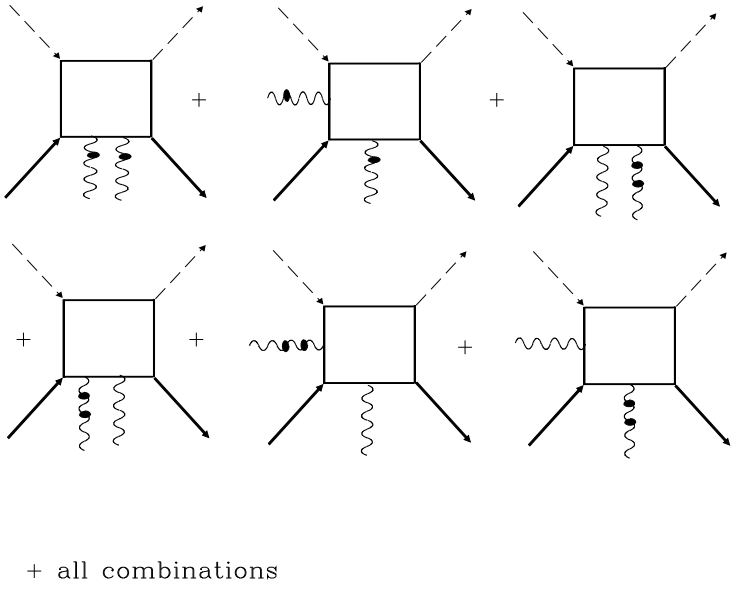

Figure 9: Diagrams of dimension 6. External lines with dots correspond to derivatives in external fields. All notations as in Fig.6

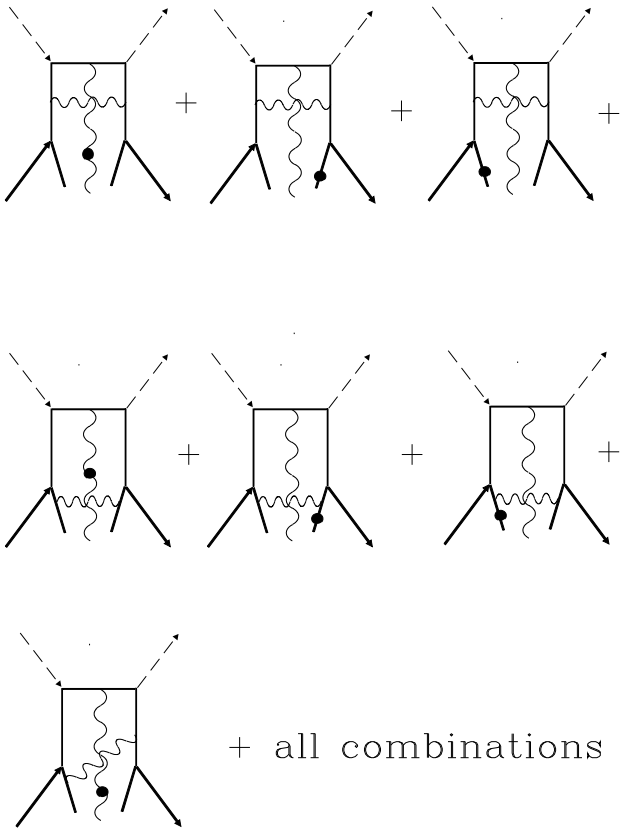

Figure 10: Diagrams of dimension 6, corresponding to the quark propagator expansion. All notations as in Fig.4

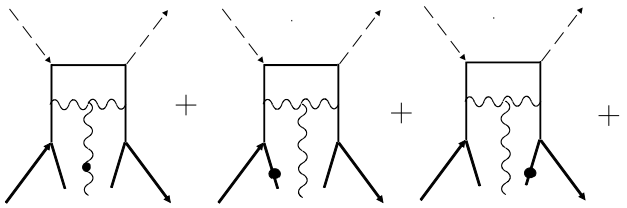

Figure 11: Diagrams of dimension 6, corresponding to the quark and gluon propagator expansion. All notations as in Fig.4

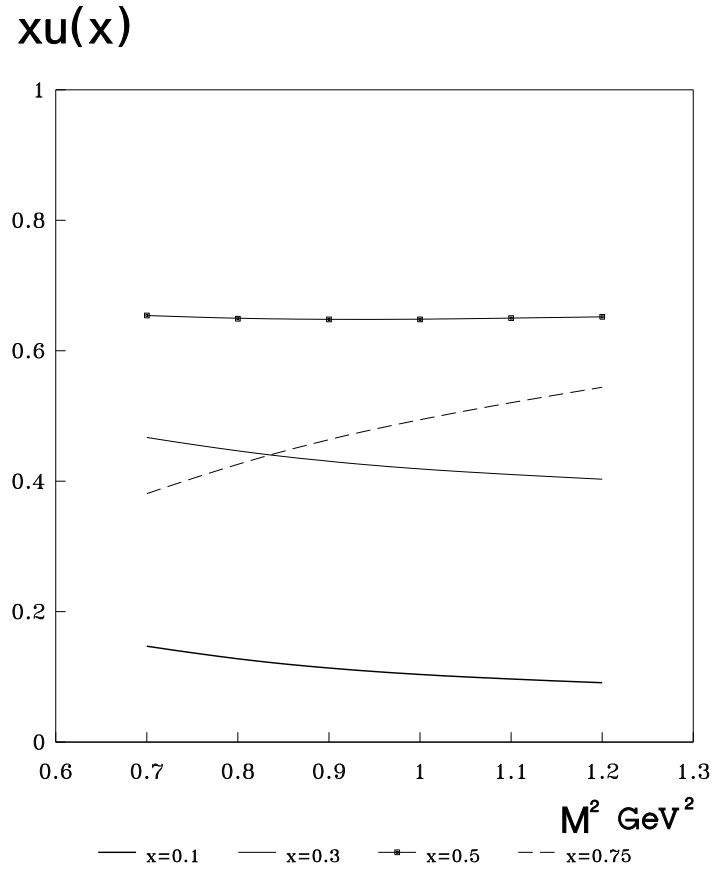

Figure 12: Borel mass dependence of the quark distribution function $xu_\rho^L(x)$ at various x

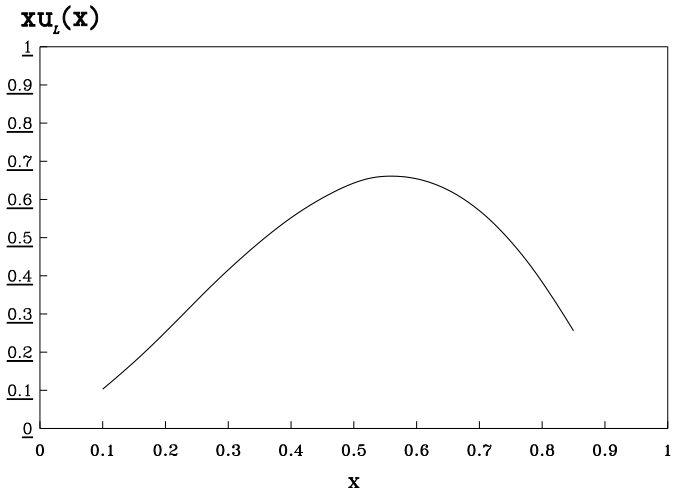

Figure 13: quark distribution function $xu_\rho^L(x)$

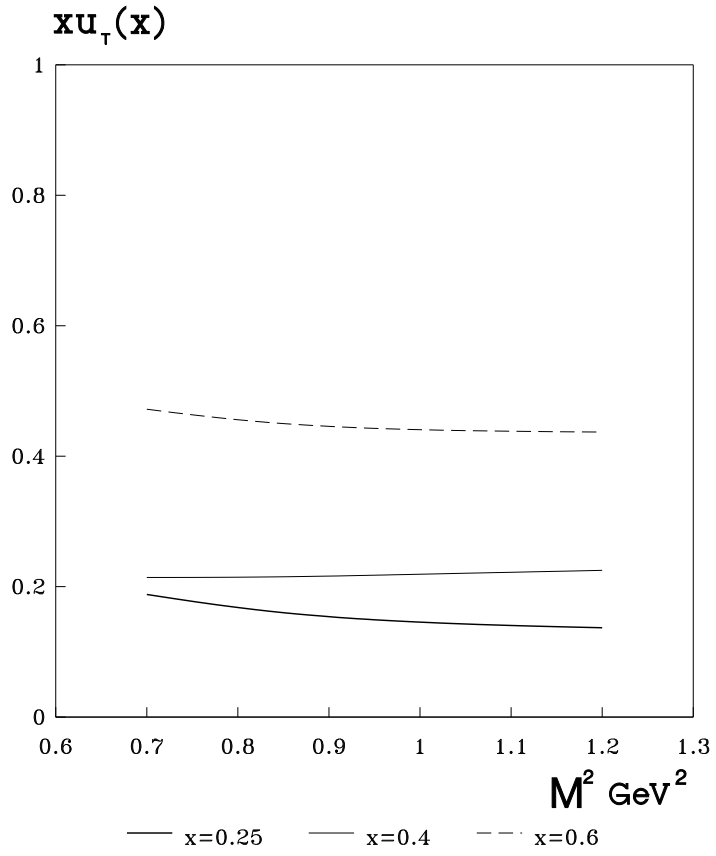

Figure 14: Borel mass dependence of the quark distribution function $xu_\rho^T(x)$ at various x

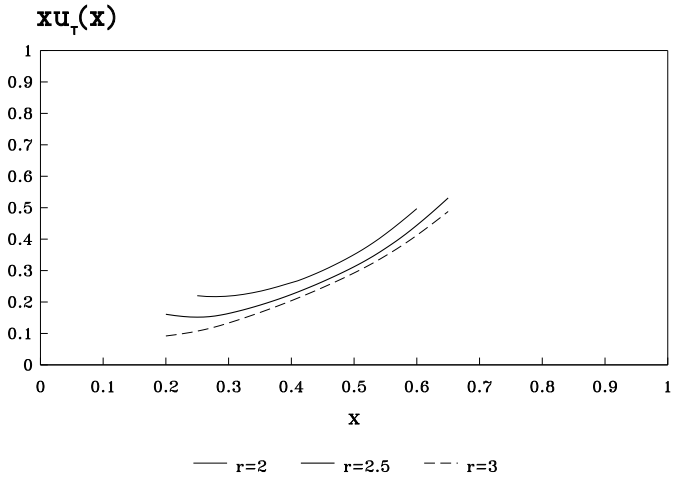

Figure 15: $xu^T(x)$ for transversally polarizied ρ-meson at three choices of instanton radius $\rho = 2, 2.5, 3\ GeV^{-1}$ (correspondingly, curves are labelled by $r = 2, r = 2.5, r = 3$)

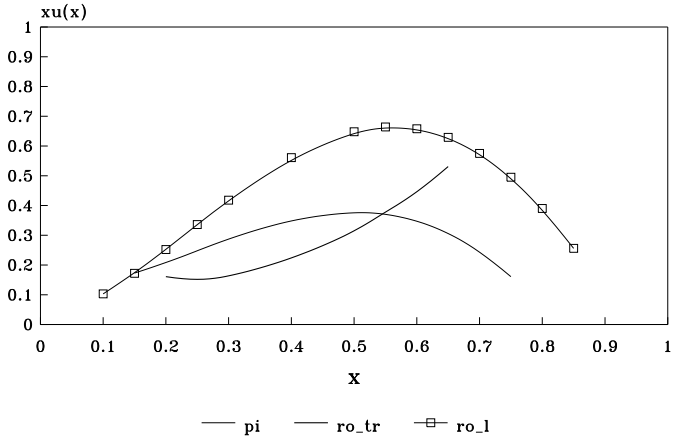

Figure 16: xu(x) for ρ^T-(curve is labelled by ro-tr), ρ^L (is labelled by ro-l) and π-meson (pi)